Magnetic properties of iron-filled multiwalled carbon nanotubes

N. Aguiló-Aguayo, J. García-Céspedes, E. Pascual and E. Bertran

FEMAN Group, IN_2UB, Departament de Física Aplicada i Òptica, Universitat de Barcelona.
C/ Martí i Franquès, 1, E-08028, Barcelona, Catalonia, Spain

ABSTRACT

Magnetic properties of iron-filled multiwalled carbon nanotubes have been investigated. Hysteretic and temperature dependent magnetic responses reveal a superparamagnetic behaviour at temperatures above 124 ºC. The saturation magnetization (M_S) of the nanowires at 5 K is found to be 152 emu/g similar to the expected bulk value of Fe_3C. Analysis of field-cooled (FC) and the zero-field-cooled (ZFC) curves show a high magnetic anisotropy of the nanowires. Langevin function has been fitted using data at 300 K. The average domain size estimated has been $V \approx 4.18 \cdot 10^{-20}$ cm^3 corresponding to spherical domains with radius $r \approx 2.2$ nm, below the value from TEM observations $r \approx 7$ nm, suggesting the presence of pseudo-single domains, with multi-domain-like and single-domain-like of radius $r \approx 2.2$ nm. The temperature dependence of coercivity give us an estimated value of blocking temperature $T_B \sim 397$ K. Possible uses of these material point to magnetic resonance imaging and other biomedical applications.

Keywords: Carbon nanotubs, magnetic properties, superparamagnetism, ZFC-FC

1 INTRODUCTION

In the last decades, superparamagnetic nanoparticles and carbon nanotubes have been a focus of interest in drug delivery, cancer treatment and diagnosis, and Magnetic Ressonance Imaging (MRI), among others novel biomedical applications.[1]

In the present article, magnetic behaviour of iron filled multiwalled carbon nanotubes has been studied from superparamagnetic approach. In addition, the structure and morphologic characteristics of iron-filled multiwalled nanotubes were determined by transmission electron microscopy (TEM) and selected area electron diffraction (SAED). The cause-effect relations with magnetic behaviour have been established.

2 EXPERIMENTAL

CNTs were produced by injection chemical vapor deposition (ICVD) using a quartz tube placed inside a tubular furnace (set up at 760 ºC) with a laminar flow of Ar dragging a precursor vapor. The substrates were copper foils of 2 x 3 cm approximately and 100 µm thick. Another small quartz substrate of 10x15x2 mm was placed together for comparison after the process. The growth precursors involved were prepared in a liquid solution of ferrocene in toluene (mass percentage of 8.76 %) and released into the tube at a constant rate of 5.6 cm^3/h. The solution was vaporised thanks to a furnace located just after the feedthrough, which is set up at 180 ºC (the vaporisation temperature of ferrocene and toluene are 175 and 110 ºC, respectively), and was carried through the main furnace by a gas mixture of Ar and H_2 ($\Phi Ar:\Phi H_2 = 250:2.5$; –flux values in standard cm^3/min–). The pressure inside the tube was slightly over atmospheric, thus a pumping system was unnecessary.

Prior to CNTs deposition on copper, a 20 nm thick TiN barrier layer was deposited by magnetron sputtering, in order to avoid catalyst diffusion.

For a full description of the experimental set-up for CNTs production and a systematic study of the different deposition parameters influence see [2].

For SEM observations, a Hitachi H-4100FE operated at 25 kV were used. A Philips CM30 operated at 300 kV was used for TEM, HRTEM and SAED structural characterisation. A superonducting-quantum-interference-device (SQUID) magnetometer was used to study the magnetic behaviour of iron-filled multiwalled carbon nanotubes in the temperature range 5-300 K and in fields up to 55 kOe.

3 RESULTS AND DISCUSSION

3.1 Structure properties

CNTs grown on TiN-coated Cu show a partial alignment perpendicular to the substrate surface, due to a crowding effect [3]. The estimated length is between 20 and 30 µm, according to SEM observations. TEM observation allowed a more accurate study of the nanostructures. In figure 1 CNTs grown on TiN-coated Cu are shown. The image reveals a concatenation of multiwalled carbon capsules.

Electron diffraction patterns obtained from small areas of the samples revealed a crystalline structure corresponding to Fe_3C (figure 1b), that is a material commonly found in CNTs synthesized by CVD [4, 5], and is associated with the deactivation of Fe as a catalyst [6, 7]. However, Fe_3C might not be the only material encapsulated inside the nanostructure bodies, as confirmed by X-ray diffraction (figure 2)**.** Because of the great amount of catalyst material encapsulated in the sample, it

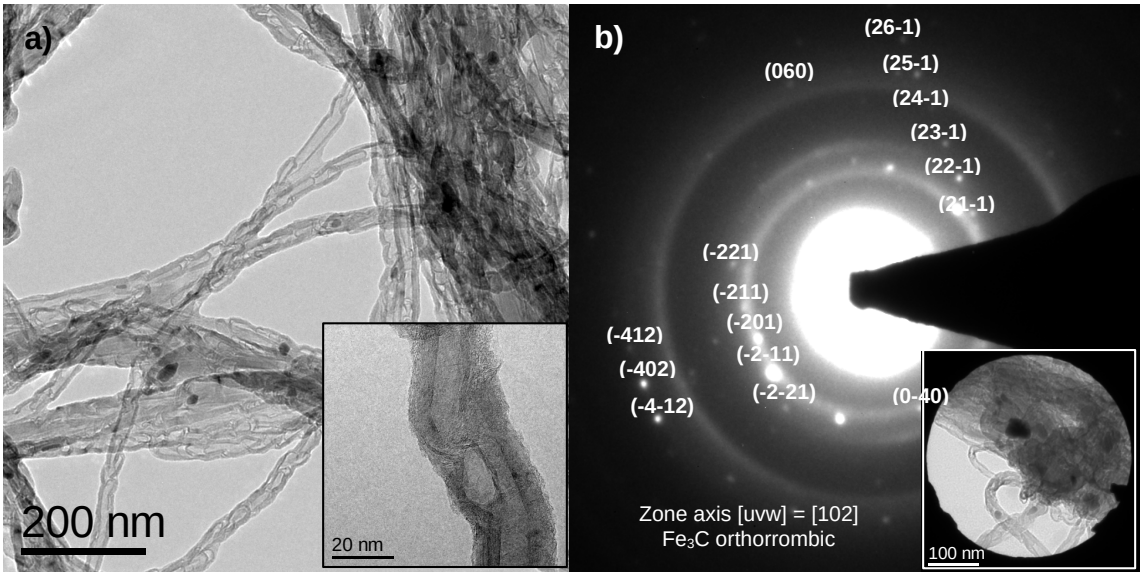

Figure 1. TEM analysis of CNTs obtained over TiN-coated Cu (a). It is observed a bamboo-like structure, with an important quantity of catalyst (iron based) material encapsulated on it. The inset in figure a) show HRTEM micrographs of the graphitic multiwalls. SAED patterns in b) are associated with the Fe_3C phases present into nanoparticles.

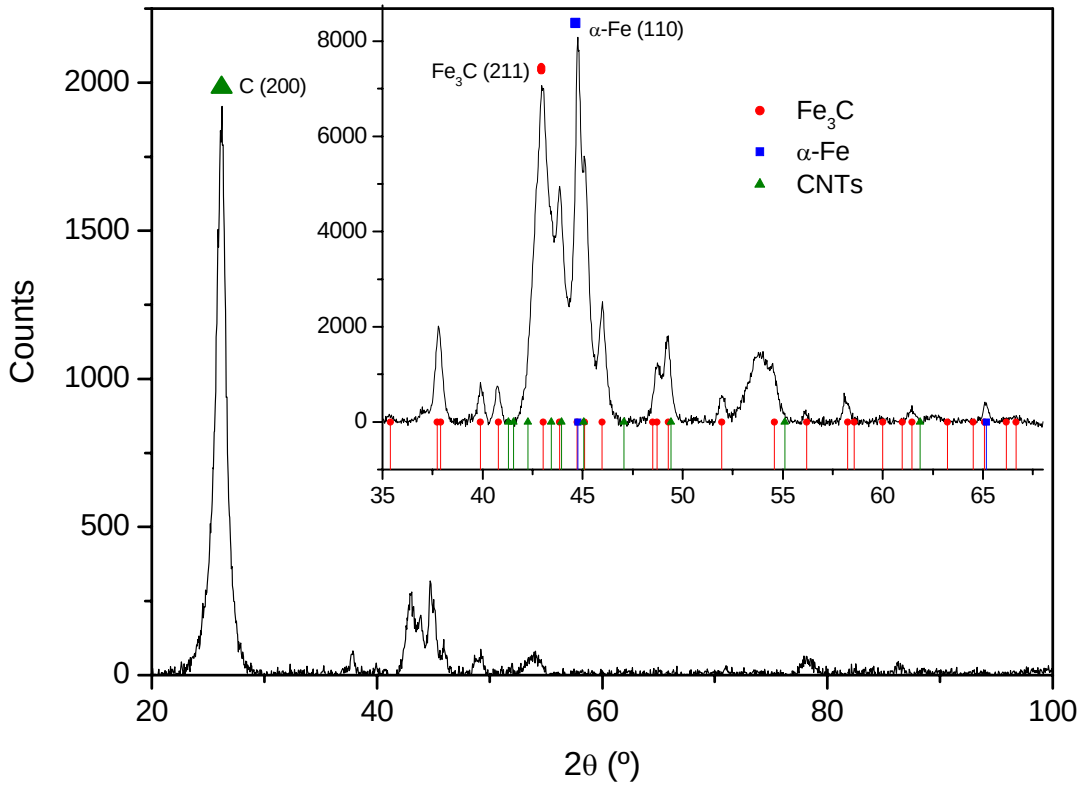

Figure 2. X-ray diffraction pattern of CNTs grown on copper. α-Fe, Fe_3C phases were found in addition to carbon phases.. Only main peaks have been labeled.

NSTI-Nanotech 2008, www.nsti.org, ISBN 978-1-4200-8503-7 Vol. 1

was possible to identify at least two different contributions among the many diffraction peaks, apart from C. The most feasible phases present into nanoparticles are Fe_3C and α-Fe (Ferrite).

3.2 Magnetic properties

Superconducting quantum interference device (SQUID) magnetometry studies have revealed the magnetic behaviour of the iron-filled multiwalled carbon nanotubes. The TEM studies have shown that the average size of the Fe grains was about 15 nm. The total mass of our sample was about ~ 85 μg. To measure it, a known mass of CNTs was oxidized in air at 600 ºC for 30 minutes, converting all the carbon material into CO_2. Then, the remaining iron oxide was weighted. From this resulting mass, the iron content was extracted by considering all the material as Fe_2O_3. The corresponding apparent saturation magnetization was 152 emu/g at 5 K, this value is similar to the estimated saturation magnetization for a bulk sample of Fe_3C (~ 169 emu/g at 0 K), since it is the most predominating component, as X-ray diffraction and SAED results had predicted.

Figures 3 shows the M(H) curves versus H at different temperatures 5, 75, 150, 225 and 300 K. As the temperature is increased, the magnetization curve exhibits less hysteresis due to the superaparamagnetic behaviour is being achieved [9]. The inset of figure 3 represents the temperature dependence of saturation magnetization (M_S) and remanent magnetization (M_r), both values are decreasing with the increase of temperature in accordance with the above mentioned.

The ZFC-FC magnetization curves are shown in figure 4. When a field of 100 Oe is applied, we observed a maximum of magnetization located above 330 K, then the blocking temperature will be situated around this value, but this method is not accurate enough to determine the specific value of blocking temperature, T_B. However, those curves give information about the anisotropy of the sample [10]. In this case, the anisotropy of the sample is low since FC magnetization remains almost constant with the temperature.

For biomedical applications, it is very interesting to know the behaviour of the magnetic nanoparticles inside the human body, so that, we will study the magnetization curve at 300 K. This curve can be fit to a Langevin function L using the following relation [11].

$$\frac{M}{M_S} = L\left(\frac{\mu H}{k_B T}\right) = \coth\left(\frac{\mu H}{k_B T}\right) - \frac{k_B T}{\mu H} \qquad (1)$$

Where M_S is the saturation magnetization, μ is the effective moment given by the product $M_S \cdot \langle V \rangle$ and $\langle V \rangle$ is the average particle volume.

The effective moment value $\mu \approx 5.44 \cdot 10^{-17}$ emu is obtained using data for 300 K and fitting magnetization by least-squares (figure 5). Using the effective moment and the known value of saturation magnetization of Fe_3C (the predominating material of our sample) at 0 K which is $\sigma_0 = 1302$ emu/cm^3 [12], we could estimate the diameter corresponding to spherical particles which is about $D \approx 4.3$ nm. This value is lower than the average size found in TEM observations, $D \approx 15$ nm, therefore, the present system suggests that we have a situation of pseudo-single domains, with regions of multi-domain-like and other regions single-domain-like of 4.3 nm with superparamagnetic behaviour.

To estimate the value of the blocking temperature, T_B, the dependence of the coercivity with temperature is plotted (figure 6). The coercivity depends on the anisotropy of the sample and its value is related with the difference between field-cooled (FC) and zero-field-cooled (ZFC) susceptibilities. We represent the coercivity H_C as the average along the positive and negative H axis, $H_C(T)=1/2(|H_{C+}|+|H_{C-}|)$, for each temperature. The temperature dependence of the coercivity is fitted by least-square to the following equation [13]:

$$H_C = H_{Ci}\left[1 - \left[\frac{T}{T_B}\right]^{1/2}\right] \qquad (2)$$

We found a zero temperature coercivity of 2792 Oe and a blocking temperature of 397 K , greater than 330 K in accordance with the ZFC-FC mesurements.

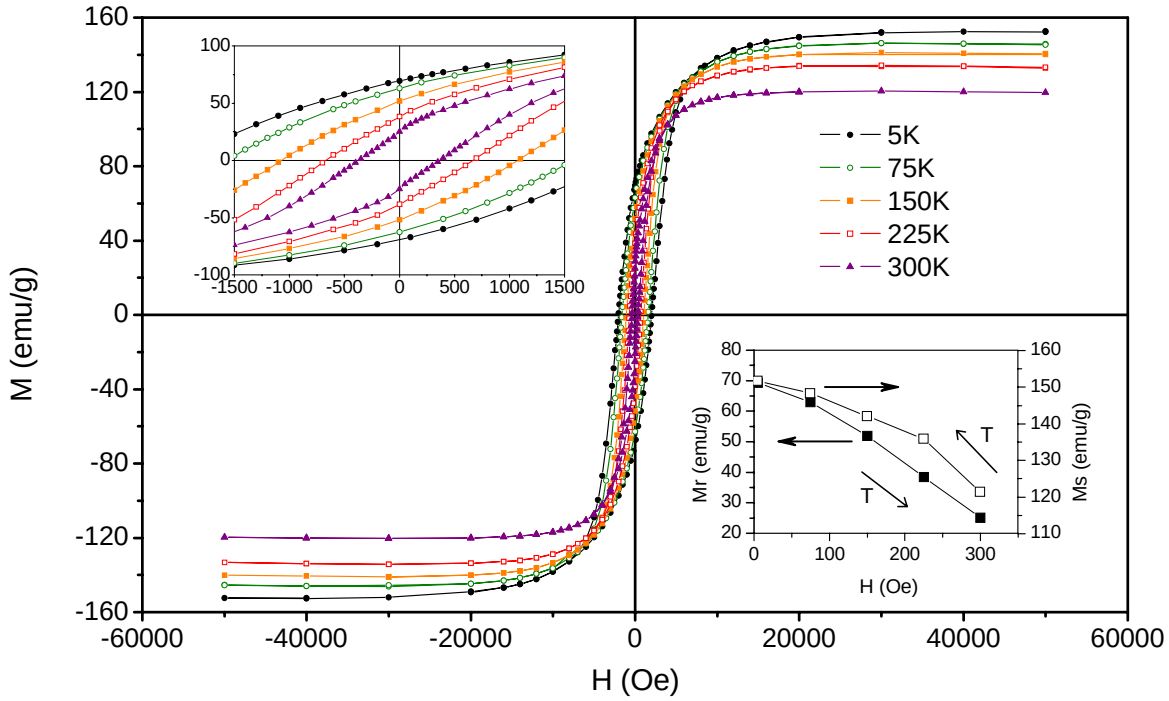

Figure 3. Magnetization versus applied field at temperatures of 5, 75, 150, 225 and 300 K for the Fe-filled MWCNTs. The inset shows the temperature dependence of remanent magnetization (close squares) and saturation magnetization (open squares) calculated from M(H) plots at different T.

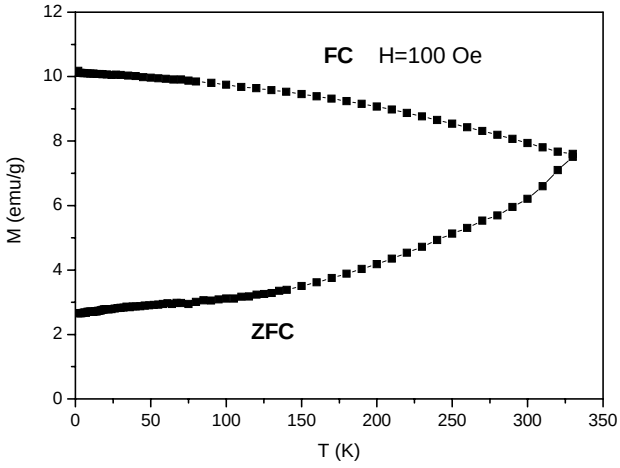

Figure 4. Magnetic susceptibility curves for ZFC and FC measured at low magnetic field of 100 Oe.

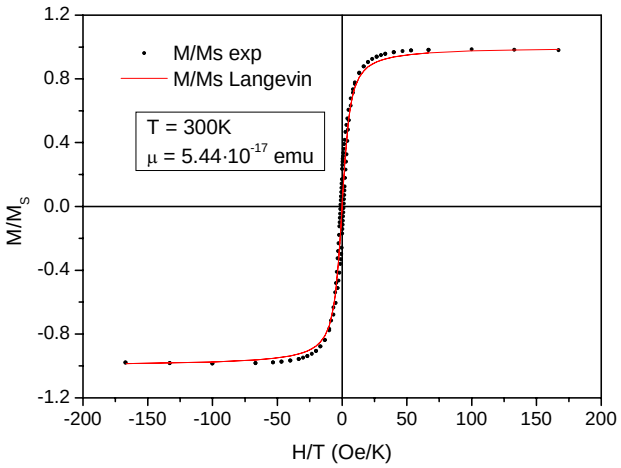

Figure 5. Magnetization versus H/T at 300 K fitted to a Langevin function, eq. (1). The effective moment found was $\mu \approx 5.44 \cdot 10^{-17}$ emu corresponding to a domain size of spherical particles with a diameter about 4.3 nm.

NSTI-Nanotech 2008, www.nsti.org, ISBN 978-1-4200-8503-7 Vol. 1

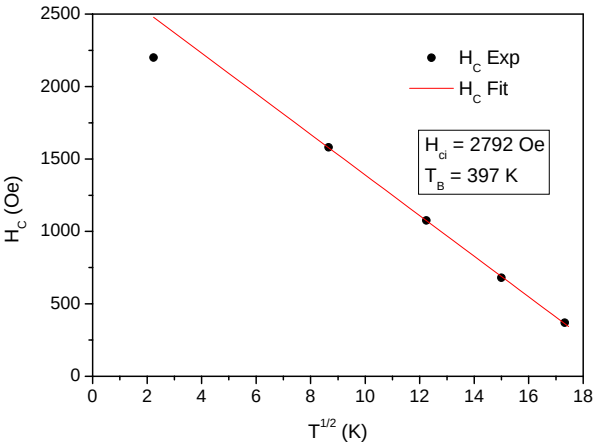

Figure 6. Temperature dependence of coercivity H_C. The H_C versus $T^{1/2}$ law was fitted to find the blocking temperature T_B.

4 CONCLUSIONS

A densely packed mat of partially aligned, bamboo-like CNTs have been grown on both faces of a TiN-coated Cu sheet, with an average size of about 30 μm, by means of ferrocene injection CVD.

Catalyst particles within CNTs have been identified as Fe_3C by SAED, although X-ray diffraction has shown other possible materials involved, as α- Fe and γ-Fe.

Magnetic properties of iron-filled multiwalled carbon nanotubes have been investigated using superconducting-quantum-interference-device magnetometry (SQUID). Hysteretic and temperature dependent magnetic responses reveal a superparamagnetic behaviour at temperatures above 397 K. The saturation magnetization is slightly different from the expected value of α-Fe due to the presence fraction of other components such as Fe_3C and γ-Fe in accordance with X-ray diffraction results. Magnetization data at 300K follows the Langevin function, which indicates that the diameter of the spherical particle domain is about 7nm, below the value from TEM observations suggesting the presence of pseudo-single domains.

5 ACKNOWLEDGMENTS

This study was supported by projects CSD2006-12 and DPI2006-03070 of MEDU of Spain. The authors thank Serveis Científico-tècnics of the Universitat de Barcelona (SCT-UB) for measurement facilities. J.G-C. thanks to Electrical Engineering and Materials Science & Metallurgy Departments of University of Cambridge for the use of their facilities for CNTs sample fabrication, specially to Prof. W.I.Milne, Dr. K.B.K.Teo and Dr. I.Kinloch.

REFERENCES

[1] C. Singh, M. S. P. Shaffer, A. H. Windle, Carbon 41, 359, 2003.
[2] C. S. S. R. Kumar, Wiley-VCH, 448, 2007.
[3] S. Fan, M. G. Chapline, N. R. Franklin, T. W. Tombler, A. M. Cassell, H. Dai, Science 283, 512, 1999.
[4] A. Oberlin, M. Endo, T. Koyama, Journal of Crystal Growth 32, 335, 1976.
[5] L. Sun, F. Banhart, Krasheninnikov, J. A. Rodríguez-Manzo, M. Terrones, P. M. Ajayan, Science 312, 1199, 2006.
[6] K. Hernadi, A. Fonseca, J. B. Nagy, D. Bernaerts, A. A. Lucas, Carbon 34 (10), 1249, 1996.
[7] S. Herreyre, P. Gadelle, P. Moral, J. M. M. Mollet, Journal of physical chemical solids 58 (10), 1539, 1997.
[8] H. Kim, M. J. Kaufman, W. M. Sigmund, Journal of Materials Research 18 (5), 1104 , 2003.
[9] D.L. Leslie-Pelecky, R. D. Rieke, Chemical Materials 8, 1770-1783, 1998.
[10] P. A. Joy, P. S. Anil Kumar, S. K. Date, Journal Physics: Condensed matter 10, 11049-11054, 1998.
[11] M. E. McHerny, S. A. Majetich, J. O. Artman, M.DeGaef, S. W. Staley, Physical Review B 49, 11358-11363, 1994.
[12] T. Mühl, D. Elefant, A. Graff, R. Kozhuharova, A. Leonhardt, I. Mönch, M. Ritsch, P. Simon, S. Groudeva-Zotova, C. M. Schneider, Journal of Applied Physics 93 (10), 7894-7896, 2003.
[13] S. Gangopadhyay, G. C. Hadjipanayis, Physical Review B 45, 9778-9787, 1992.